Fall 2018

Universal wavefront transmission through disordered media

Jayson Robert Summers

UNIVERSAL WAVEFRONT TRANSMISSION THROUGH DISORDERED MEDIA

by

JAYSON ROBERT SUMMERS

A THESIS

Presented to the Graduate Faculty of the

MISSOURI UNIVERSITY OF SCIENCE AND TECHNOLOGY

In Partial Fulfillment of the Requirements for the Degree

MASTER OF SCIENCE

in

PHYSICS

2018

Approved by

Alexey Yamilov, Advisor
Jerry Peacher
Daniel Fischer

ABSTRACT

When electromagnetic waves propagate through random dielectric media, they scatter in a predictable, deterministic way. The process is also fully reversible. If one sends an exiting wave backward through the same material, it will converge back to its original form and location in the same amount of time it took to originally propagate through the material. Due to this predictability, a great deal of research has went into studying these scattering processes in multimode fibers, diffusers, biological tissues, and other media. Scientists have turned random scattering material into focusing lenses, image transmitters, and highly transmitting media by controlling the impinging wavefronts with Spatial Light Modulators (SLMs).

The purpose of this work is to determine whether or not there is “one size fits all" impinging waveform which, assuming nothing is known about the material, is your best bet for maximum transmission. If such a waveform existed, researchers would no longer need to measure the materials’ transmission matrix, optimize waveforms, measure complex interference patterns, or invasively embed local sensors into the system. Using a combination of iterative feedback and transmission matrix approaches, we devised an algorithm which computed this average wavefront for several different systems, concluding that the best average transmission takes place when maximum flux is placed upon the path of least resistance, similar to electronic conduction.

ACKNOWLEDGMENTS

I would first like to thank my thesis advisor, Dr. Alexey Yamilov, of Missouri University of Science and Technology. Without his kindness and patience, this thesis would have never been completed. He has always had a magical ability to tie difficult large-scale concepts together while still carefully explaining every mathematical detail to me. In the beginning, much of this material was confusing and daunting, but now looking back I can see how Dr. Yamilov was guiding me along the way, breaking the work into easily digestible pieces which I was ready for at the time. I'm sincerely grateful to him and find it difficult to imagine a better person to have worked with.

I would like to further thank Dr. Jerry Peacher and Dr. Daniel Fischer for serving on my thesis committee and offering their valuable time and input into this work. Without their participation and input, there would have been no way to validate this work. Their valuable expertise and contributions are greatly appreciated.

Finally, I would like to thank my parents for their support and encouragement over the years, never failing to remind me that all things are possible if you believe and put in the work. Thank you.

TABLE OF CONTENTS

Page

LIST OF ILLUSTRATIONS

1. INTRODUCTION

1.1. WAVE PROPAGATION IN FREE SPACE AND IN WAVEGUIDES

Plane Waves. A wave front can be defined as the locus of points in space which are all identical in their phase of oscillation. The simplest three-dimensional wave is the plane wave, which travels in a direction perpendicular to the wave-fronts. The one dimensional wave equation describing it is well known

$$\frac{\partial^2 \psi}{\partial t^2} = v^2 \frac{\partial^2 \psi}{\partial z'^2}. \tag{1.1}$$

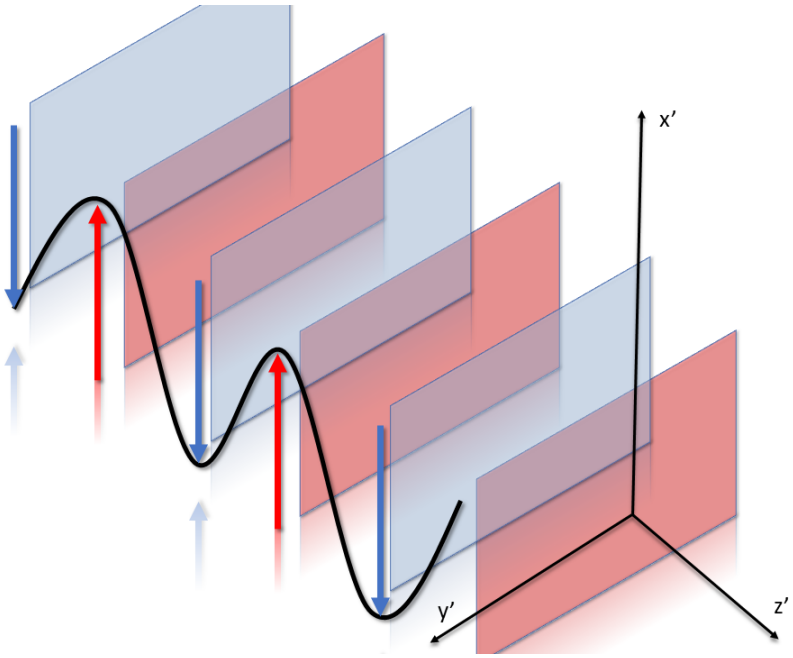

Figure 1.1. Plane Wave Moving Along The z' Axis.

Equation 1.1 is a partial differential equation of second order. For the axes pictured in Figure 1.1, it has the well known solution $\psi = \psi_0 \cos(\omega t - kz' + \phi)$. This is a wave propagating in the z' direction with a phase velocity v equal to ω/k. Each wavefront is a geometrical surface in the x'-y' plane with a phase equal to $\omega t - kz' + \phi$, which is a constant everywhere in that plane.

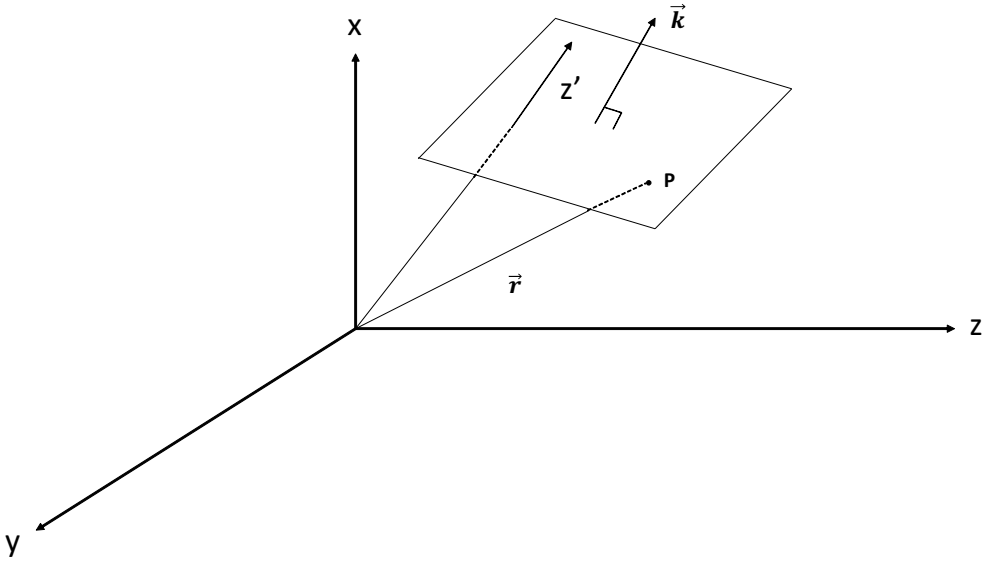

Figure 1.2. Plane Waves Moving Along z' Axis.

The Wave Vector k. A plane wave can be chosen to propagate in an arbitrary direction. We will now express the same wavefront $\psi = \psi_0 \cos(\omega t - kz' + \phi)$ in the new coordinate system x, y, z as displayed in Figure 1.2. Let the position point P be represented by the vector $\vec{r} = x\hat{x} + y\hat{y} + z\hat{z}$, where $\hat{x}, \hat{y}, \hat{z}$ are the unit vectors along each axis. The wavefront can now be expressed as $\psi = \psi_0 \cos(\omega t - k(\vec{r} \cdot \hat{z}') + \phi)$. This follows from the fact that $z' = r\cos(\theta) = \vec{r} \cdot \hat{z}'$, where θ is the angle between $\vec{r}$ and $\hat{z}'$. Now we will manipulate the $k(\vec{r} \cdot \hat{z}')$ term as

$$k(\vec{r} \cdot \hat{z}') = (k\hat{z}') \cdot \vec{r}. \tag{1.2}$$

The product $k\hat{z}'$ is a vector lying in the propagation direction $\vec{z}'$ having a magnitude equal to $k = \omega/v$. This vector $\vec{k}$ is called the wave vector. Now we can rewrite the plane wave as follows

$$\begin{aligned} \psi &= \psi_0 \cos(\omega t - \vec{k} \cdot \vec{r} + \phi) \\ &= \psi_0 \cos(\omega t - (k_x x + k_y y + k_z z) + \phi) \end{aligned} \tag{1.3}$$

where $\vec{k} = k_x\hat{x} + k_y\hat{y} + k_z\hat{z}$ and $k = \sqrt{k_x^2 + k_y^2 + k_z^2}$. The terms k_x, k_y, k_z are equal to the number of radians of phase change per unit displacement along the x, y, and z axes. Thus the absolute value of $|\vec{k}|$ is related to the wavelength as $2\pi/\lambda$.

The Three Dimensional Wave Equation. The three dimensional wave equation is very similar to its one dimensional counterpart Equation 1.1. It can be written in Cartesian coordinates as (Bekefi and Barrett, 1977)

$$\frac{\partial^2\psi}{\partial t^2} = v^2\left(\frac{\partial^2\psi}{\partial x^2} + \frac{\partial^2\psi}{\partial y^2} + \frac{\partial^2\psi}{\partial z^2}\right) = v^2\nabla^2\psi \tag{1.4}$$

where ∇ is the gradient operator and ∇^2 is the Laplace operator. As a quick exercise, we will verify that Equation 1.3 is indeed a solution to Equation 1.4. First doing the time derivative we arrive at $\partial^2\psi/\partial t^2 = -\omega^2\psi$. Next we take the spatial derivatives and arrive at $\left(\frac{\partial^2\psi}{\partial x^2} + \frac{\partial^2\psi}{\partial y^2} + \frac{\partial^2\psi}{\partial z^2}\right) = -\left(k_x^2 + k_y^2 + k_z^2\right)\psi$. Putting it all together

$$\omega^2\psi = v^2\left(k_x^2 + k_y^2 + k_z^2\right)\psi. \tag{1.5}$$

Noting that $(vk)^2 = \omega^2$, we see that the equation balances correctly. Equation 1.5 is known as the dispersion equation.

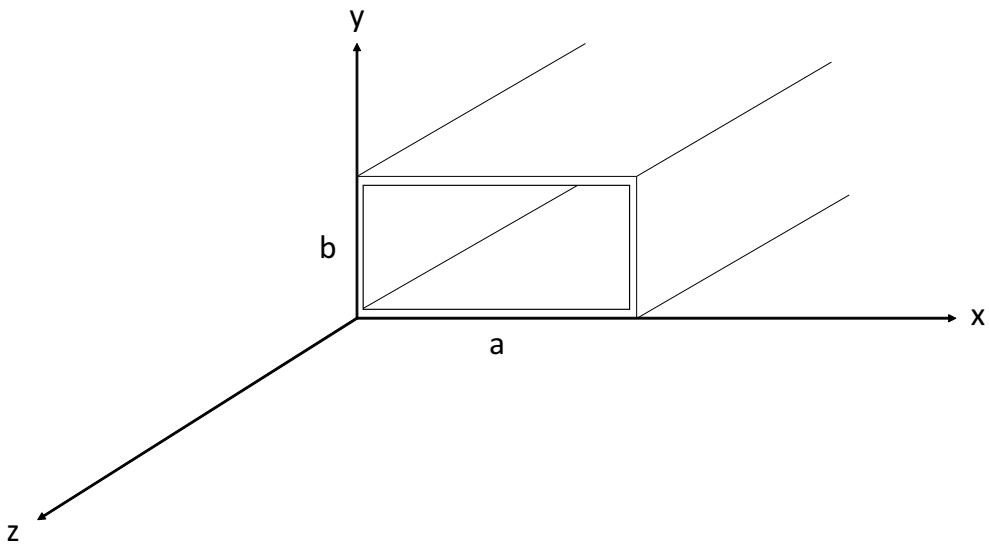

Figure 1.3. A Rectangular Waveguide. The electric field vector is oriented along the y axis.

A Rectangular Waveguide And Its Modes. Throughout this work, we will be studying the transmission of plane waves through dielectric media sandwiched inside of a waveguide (Bekefi and Barrett, 1977), so it is worth our time to go over wave transmission in a waveguide. In this section we will discuss the rectangular waveguide depicted in Figure 1.3.

First off, assume that the mode of propagation has an electric field vector that is entirely along the y axis, $\vec{E} = E_y\hat{y}$, and that it is uniform in the y direction. According to the boundary conditions, E_x must be zero at the top ($y = b$) and bottom ($y = 0$) of the waveguide, and $E_y = 0$ at both of the sides $x = 0$ and $x = a$. Considering $\vec{E}$ is entirely in the y direction, we have no problems with $E_x = 0$ at $y = 0$ and $y = b$, but in the x-direction there are many periodic functions available to us, so we will let E_y be proportional to some unknown function $g(x)$. Also, since this wave will be traveling along the z-axis, it will also be proportional to $exp(i\omega t - ik_z z)$, where k_z is the propagation constant of the wave,

another quantity which we must determine. So we can now write,

$$E_y = g(x)e^{i(\omega t - k_z z)} \tag{1.6}$$

E_y must also be a solution of the three-dimensional wave equation

$$\frac{\partial^2 E_y}{\partial x^2} + \frac{\partial^2 E_y}{\partial y^2} + \frac{\partial^2 E_y}{\partial z^2} = \frac{1}{c^2}\frac{\partial^2 E_y}{\partial t^2}. \tag{1.7}$$

Inserting Equation 1.6 into Equation 1.7 and doing a bit of manipulation, we arrive at the following,

$$\left[\frac{\partial^2 g}{\partial x^2} + \left(\frac{\omega}{c}\right)^2 g - k_z^2 g\right] e^{i(\omega t - k_z z)} = 0. \tag{1.8}$$

Equation 1.8 can only be satisfied if the term in square brackets is zero.

$$\frac{\partial^2 g}{\partial x^2} + \left[\left(\frac{\omega}{c}\right)^2 - k_z^2\right] g = 0. \tag{1.9}$$

This differential equation has a simple solution.

$$\begin{aligned} g(x) &= A\cos(k_x x) + B\sin(k_x x) \\ k_x &= \pm\sqrt{\left(\frac{\omega}{c}\right)^2 - k_z^2}. \end{aligned} \tag{1.10}$$

Considering our boundary conditions earlier, we know that E_y must equal zero at $x = 0$ and $x = a$, so the same must apply to $g(x)$. This means that the constant A must be zero, and that $k_x = m\pi x/a$, where m is a positive integer. Now $g(x) = B\sin(m\pi x/a)$. Putting it all together, and remembering that the electric field is a real physical quantity, we arrive at:

$$\begin{aligned} E_y &= E_{0y}\sin(m\pi x/a)\cos(\omega t - k_z z) \\ k_z^2 &= \left(\frac{\omega}{c}\right)^2\left[1 - \left(\frac{m\pi c}{\omega a}\right)^2\right] \end{aligned} \tag{1.11}$$

Analysis of this equation shows that there exists a maximum $m_{max} = \frac{\omega a}{\pi c} = \frac{a}{\lambda/2}$.

1.2. DETERMINISM OF WAVE PROPAGATION AND SHAPING TECHNIQUES

When an electromagnetic wave propagates through a medium containing random scatterers, such as that found within a disordered dielectric medium, the wave output will often look completely random, lacking any recognizable pattern (Goodman, 2010). However, this sort of process is not actually random. Random implies that one cannot know the outcome and that one can only predict the result with a given probability, such as drawing a card from a deck. In this case, it's more proper to say that the outcome is complicated and difficult to predict, yet it is deterministic (Freund, 1990; Kramer, 1996). Given a system of scatterers and a wavefront impinging on a system, there is only one way that the light will scatter throughout the material each and every time. Not only this, the process is also reversible. If you send the scattered waves back through the material from wherever they emerged, they will converge back to their original source. This is a consequence of the fact that the wave equation is of the second order in time, so that reversing time in any solution is automatically a solution (Beenakker, 1997; Fink, 1997).

Over the last fifty years, much research has gone into studying these scattering processes, giving scientists a great deal of control of these electromagnetic waves in multimode fibers, diffusers, biological tissue, and other mediums (Mosk *et al.*, 2012). It turns out that if one can create and control the impinging wavefront, a seemingly random scattering material can act as a focusing lens, transmit images, or even make a scattering medium transmit 100% of the incident light (Mosk *et al.*, 2012). These wavefronts are created using a technique called wavefront shaping, and are achieved using devices called Spatial Light Modulaters (SLMs). These devices can rapidly produce arbitrary wavefronts by manipulating liquid crystal technology by computer.

Now that we have a method of creating the impinging wavefront, the next question becomes how to determine the correct wavefront for our particular goal. Say we desire the wavefront with the maximal transmission through a material, or we wish to use the material as a lens and focus our waves to a particular point. How would one go about determining the needed wavefront? In general, there are three different methods. The first technique relies on iterative feedback schemes (Vellekoop, 2015; Vellekoop and Mosk, 2007). You place a feedback sensor at the position of the desired focus, and you keep modifying the wavefront using the SLM and computer software algorithms, optimizing and tweaking until you finally find the proper wavefront. This method is frequently used to quickly focus light at a particular location through a material. The second technique is called digital optical phase conjugation (Fink *et al.*, 2000; Yaqoob *et al.*, 2008). It uses interferometry to measure light scattered within the material, and these patterns are used to send light back through the material using a SLM, essentially reversing the scattering process. This is possible because wave propagation is completely reversible. This technique can produce images in the sub-millisecond scale, making it applicable to imaging biological tissue, though it requires coherent light sources for proper reversal. A third category of techniques relies on what's called the transmission matrix (Popoff *et al.*, 2010, 2011). A transmission matrix treats the medium as a black box, relating an incoming wave and the scattered wave. To find this matrix, one must measure the scattered light's amplitude and phase, making it also rely on interferometry. This can be difficult experimental work, so to simplify matters, there have been computational algorithms devised which can infer phase from a pair of spatial intensity measurements.

1.3. GOALS AND MOTIVATION

The central purpose of this work is to determine whether or not there is “one size fits all" waveform which, assuming you know absolutely nothing about the system, is your best bet for maximum transmission. If such a waveform exists, it could save one from much of the experimental complications of measuring the transmission matrix, optimizing waveforms, introducing local sensors, or making complicated interference measurements. To pursue this goal, we will be utilizing two of the three wave shaping techniques just discussed. First we will be simulating wave propagation through thousands of random dielectric waveguides using a computational library called KWANT (Groth *et al.*, 2014). This library will allow us to compute the transmission matrix for each of these systems, and we will then use these, along with an iterative computational algorithm, to find a universal wavefront which has maximum average transmission throughout all systems.

2. SCATTERING MATRIX FORMALISM

As has been previously mentioned, the KWANT system was used to perform many of the calculations involved in this project. Kwant uses the scattering-matrix formalism for its internal bookeeping, so this section's purpose is to introduce the reader to this approach.

2.1. HISTORY AND APPLICATION OF SCATTERING MATRIX FORMALISM

The earliest beginnings of the scattering matrix date back to 1937 when John Archibald Wheeler used it to describe the physics of light nuclei in his paper "On the Mathematical Description of Light Nuclei by the Method of Resonanting Group Structure" (Wikipedia, 2018a). A unitary matrix of coefficients was used to connect "the asymptotic behaviour of an arbitrary particular solution [of the integral equations] with that of solutions of the standard form", but the technique was never developed fully (Wikipedia, 2018a).

A few years later in 1940, Werner Heisenberg developed this same technique, independently, when tackling divergence problems in quantum field theory. Today the S-Matrix shows up in many areas including conformal field theory, integrable systems, quantum field theory, and string theory. For example, in high energy physics, we need to compute the probability of different outcomes in scattering problems. The scattering matrix relates the incoming particles with the probabilities that they will transform into different outgoing particles with different energies (Beenakker, 1997; Wikipedia, 2018a).

In optics, the scattering matrix is directly related to another technique called the "transfer-matrix" method. This method exploits the fact that when using Maxwell's equations, there are very simple continuity conditions for the electric and magnetic fields at the boundaries between media. If one knows the fields before a particular medium layer, using a simple matrix operation, one can know the fields at the end of the layer. Even more conveniently, these layers "stack", so if you put a number of different layers of material

together, you simply do a series of matrix multiplications to compute the total transfer matrix for the entire system. There are then simple mathematical operations which convert this transfer-matrix into the reflection and transmission components, which can be used to create the scattering matrix (Wikipedia, 2018b; Yeh, 2005).

So as can be seen, the scattering matrix approach is used in many areas of mathematics and physics.

2.2. MATHEMATICAL FORMALISM AND PROPERTIES

For us, the primary goal of this formalism is to relate the incoming flux waves impinging on the system with those scattered waves which transmit through the system. This is done using matrices and vectors. The incoming and outgoing flux waves are both represented by vectors, where the vector components are expansion coefficients in a particular set of basis waves. These basis waves are illustrated in blue in Figure 2.1. But how exactly is a wave's "flux" defined? In this formalism, the sum of the squared magnitude of the wave vector's components represent its flux.

$$\begin{aligned} \text{Incoming Flux} = \phi^{(in)} &= \sum_n |C_n^{(in)}|^2 = |\vec{C}^{(in)}|^2 \\ \text{Outgoing Flux} = \phi^{(out)} &= \sum_n |C_n^{(out)}|^2 = |\vec{C}^{(out)}|^2 \end{aligned} \tag{2.1}$$

Next off, incoming and outgoing wave vectors are related by a scattering matrix, whose components represent the transmission and reflection of each incoming mode, from the left and the right. As for notation, (l) and (r) represent waves from the left and the right, and (+) an (-) correspond to right-moving and left-moving waves.

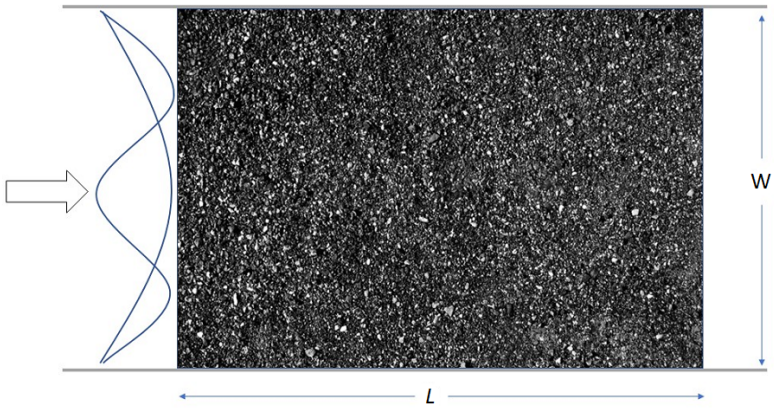

Figure 2.1. A Two-Dimensional Scattering System Inside A Waveguide.

$$\begin{aligned} \vec{C}^{(out)} &= \hat{S}\vec{C}^{(in)} \\ \text{where: } \vec{C}^{(in)} &= \begin{pmatrix} \vec{C}_l^{+} \\ \vec{C}_r^{-} \end{pmatrix}, \vec{C}^{(out)} = \begin{pmatrix} \vec{C}_l^{-} \\ \vec{C}_r^{+} \end{pmatrix} \\ \hat{S} &= \begin{pmatrix} \hat{r} & \hat{t}' \\ \hat{t} & \hat{r}' \end{pmatrix} \end{aligned} \tag{2.2}$$

Within the scattering matrix $\hat{S}$, r_{mn} corresponds to reflection amplitudes for incoming modes from the left, r'_{mn} are from the right. Likewise, t_{mn} are transmission amplitudes for incoming modes from the left, and t'_{mn} are from the right. In Figure 2.1, the basis waves are simple sin() waves of the form $X_n(y) = \sqrt{\frac{2}{W}}\sin(\frac{n\pi y}{W})$. Note that this scattering matrix is primarily a bookkeeping tool, where the medium is a black-box, which says that if you excite this system with a certain wavefront, it will transmit and reflect in such and such a way. It doesn't tell us how, or why, but just that it does.

Two quantities which are of particular interest are the total transmission, as well as total reflection. They are computed from sums of the transmission and reflection matrix elements.

$$\begin{aligned} T_n &= \sum_m |t_{mn}|^2 \\ R_n &= \sum_m |r_{mn}|^2 \end{aligned} \tag{2.3}$$

The n subscript designates the transmission or reflection of “channel" n. What does this mean? It is worth discussing briefly. Each entry within the transmission and reflection matrix has a direct physical meaning. In particular, the squared magnitude of each matrix element represents a wave flux percentage. For example, entry t_{12} designates the amount of the input wave’s basis mode 2 contribution that makes it into the output wave’s mode 1 contribution. Likewise, the entry t_{mn} designates the amount of the input wave’s basis mode n contribution that transmits through the system into the mode m contribution of the output wave. The exact same idea applies to the reflection matrix. So, if one sums over all modes n, remembering that these are flux percentages, one gets the total transmission or reflection of an input mode n in the total output wave.

Since understanding this point is crucial to understanding this project, let’s do a very simple example. Say we are examining the transmission of a simple wave through a 2D disordered system, similar to that shown in Figure 2.1. We will represent our impinging input wave, as well as the output wave, as some simple linear combination of $X_n(y)$ functions, just like in the figure, where each basis function has a different spatial frequency. For simplicity, we’ll only use three basis functions. We’ll call the amplitudes of the input wave I_1, I_2, I_3, and the output wave’s amplitudes O_1, O_2, O_3. So the input and output waves, along with the transmission matrix, look like this.

$$\begin{pmatrix} O_1 \\ O_2 \\ O_3 \end{pmatrix} = \begin{pmatrix} t_{11} & t_{12} & t_{13} \\ t_{21} & t_{22} & t_{23} \\ t_{31} & t_{32} & t_{33} \end{pmatrix} \begin{pmatrix} I_1 \\ I_2 \\ I_3 \end{pmatrix} \tag{2.4}$$

To further illustrate, let's expand this out into a set of equations.

$$\begin{aligned} O_1 &= t_{11}I_1 + t_{12}I_2 + t_{13}I_3 \\ O_2 &= t_{21}I_1 + t_{22}I_2 + t_{23}I_3 \\ O_3 &= t_{31}I_1 + t_{32}I_2 + t_{33}I_3 \end{aligned} \tag{2.5}$$

As can be seen in the equations, I_1, which is the input wave's mode one contribution, gets distributed into O_1, O_2, O_3 according to the weights t_{11}, t_{21}, t_{31}. This is a physical wave, and considering there's no absorption or gain, this influx must go somewhere, either being transmitted through or reflected. A certain percentage of this wave flux goes into O_1, a certain percentage into O_2, and a certain percentage into O_3. This sum must equal the total amount of the input wave's mode one that was transmitted into the output wave, somewhere, somehow. Do this exact same process for reflection. If you sum the squared amplitudes of t_{11}, t_{21}, t_{31} and r_{11}, r_{21}, r_{31}, you have to get 1, or 100%, because this input wave's I_1 contribution had to go somewhere, either into the transmitted or reflected wave, distributed among the corresponding output transmission and reflection vector weights.

As was mentioned earlier, in this project we're examining scattering within lossless systems contained within a waveguide, so the wave must either be transmitted or reflected without absorption or gains; therefore there must be a conservation of wave flux. This leads us to the following equations, which our discussion earlier should justify:

$$\begin{gathered} T_n + R_n = 1 \\ \sum_n (T_n + R_n) = N \\ \text{where } T_n = \sum_{m=1}^{N} |t_{mn}|^2 \text{ and } R_n = \sum_{m=1}^{N} |r_{mn}|^2 \end{gathered} \tag{2.6}$$

If one sums over all channels, $\sum_n T_n$, one is left with the total transmission T. Just as a side note, when examining electron scattering in quantum mechanical systems, there is similar quantity called the conductance, typically denoted by G, which only differs from to the total optical transmission by a constant, $G = \left(\frac{2e^2}{h}\right) T$ (Eric Akkermans, 2011).

Before moving on, it must be noted that in lossless systems, the scattering matrix must always remain unitary. This is important because later on we will devise an algorithm to optimize transmission by computing a new set of optimal basis functions, but in doing so we must always ensure that our transformation matrix also remains unitary. Why? We must retain a conservation of flux. This can be proven very easily.

$$\text{Incoming Flux} = \text{Outgoing Flux}$$

$$\phi^{(in)} = \phi^{(out)} \tag{2.7}$$

$$|\vec{C}^{(in)}|^2 = \vec{C}^{(in)\dagger}\vec{C}^{(in)} = |\vec{C}^{(out)}|^2 = \vec{C}^{(out)\dagger}\vec{C}^{(out)}$$

Now if we substitute in $\vec{C}^{(out)} = \hat{S}\vec{C}^{(in)}$ and $\vec{C}^{(out)\dagger} = \vec{C}^{(in)\dagger}\hat{S}^\dagger$, we arrive at $\vec{C}^{(in)\dagger}(\hat{S}^\dagger\hat{S} - 1)\vec{C}^{(in)} = 0$, implying that $\hat{S}^\dagger\hat{S} = 1$, or that the scattering matrix $\hat{S}$ is unitary.

3. RELATIONSHIP BETWEEN EM AND QM

As was mentioned in the introduction, the simulations used in this project relied on computations provided by the KWANT system, which is a quantum transport library. However, the focus of this research project is the optimal transmission of electromagnetic waves by manipulating optical wave-fronts impinging on a disordered medium. So the question becomes: How can a quantum mechanics library be used to solve a problem in optics? The key is to focus on only one particular component of the electric or magnetic field, say the z-component of $\vec{E}$. When doing so, the general form of the electromagnetic wave equation and the Schrodinger equation become one and the same. The purpose of this section is to show this relationship, first by deriving the electromagnetic wave equation from Maxwell's equations, and then directly showing that this equation has the same general form as Schrodinger's equation.

3.1. DERIVATION OF THE ELECTROMAGNETIC WAVE EQUATION

In our simulations, electromagnetic waves will be traveling through inhomogenous dielectric mediums. A dielectric material is an electrical insulator that can be polarized by electric fields. In a conductor, these fields would cause charge to flow across the material. However, in a dielectric material, the passing electric field causes the material's internal electron clouds to slightly shift their average equilibrium positions. These shifts create fields within the material itself which only partially cancel the electromagnetic wave passing through it. This internal resistance to forming an electric field within the material is called the permittivity. In our experiments, what varies from place to place within the medium is the electrical permittivity. With all that said, our theoretical model begins with Maxwell's equations, source-free, in a linear, frequency independent dielectric medium,

with a const dielectric permittivity $\varepsilon = constant$.

$$\begin{aligned} \nabla \cdot \vec{E} &= 0 \\ \nabla \cdot \vec{B} &= 0 \\ \nabla \times \vec{E} &= -\frac{\partial \vec{B}}{\partial t} \\ \nabla \times \vec{B} &= \mu\varepsilon \frac{\partial \vec{E}}{\partial t} \end{aligned} \tag{3.1}$$

Next we take the curl of the curl equations, assuming ε and μ are constants,

$$\begin{aligned} \nabla \times (\nabla \times \vec{E}) &= -\frac{\partial}{\partial t}(\nabla \times \vec{B}) = -\mu\varepsilon \frac{\partial^2 \vec{E}}{\partial t^2} \\ \nabla \times (\nabla \times \vec{B}) &= \mu\varepsilon \frac{\partial}{\partial t}(\nabla \times \vec{E}) = -\mu\varepsilon \frac{\partial^2 \vec{B}}{\partial t^2} \end{aligned} \tag{3.2}$$

Finally we utilize the vector identity $\nabla \times (\nabla \times \vec{V}) = \nabla(\nabla \cdot \vec{V}) - \nabla^2 \vec{V}$ remembering that $\nabla \cdot \vec{E} = \nabla \cdot \vec{B} = 0$ to arrive at the familiar electromagnetic wave equations.

$$\begin{aligned} \mu\varepsilon \frac{\partial^2 \vec{E}}{\partial t^2} - \nabla^2 \vec{E} &= 0 \\ \mu\varepsilon \frac{\partial^2 \vec{B}}{\partial t^2} - \nabla^2 \vec{B} &= 0 \end{aligned} \tag{3.3}$$

3.2. SCHRODINGER'S EQUATION AND THE EM WAVE EQUATION

We will now demonstrate that Schrodinger's equation takes on the same form as the electromagnetic wave equation, specifically when we relate stationary quantum states to monochromatic optical states. Let us begin with Schrodinger's equation.

$$\left(\frac{\vec{p}^2}{2m} + V(\vec{r}) \right) \psi(\vec{r}, t) = i\hbar \frac{\partial \psi(\vec{r}, t)}{\partial t} \tag{3.4}$$

If we consider only stationary states with well defined real energy $E = \hbar\omega$ and time-evolution $\exp(-i\omega t)$, we will arrive at the time-independent Schrodinger equation (TISE).

$$\begin{gathered}\left[\nabla^2 - \frac{2m}{\hbar^2}(V(\vec{r}) - E)\right]\psi(\vec{r}) = 0 \\ \text{where } \int d\vec{r}\psi_m^*(\vec{r})\psi_n(\vec{r}) = \delta_{mn}\end{gathered} \tag{3.5}$$

Note that the energy eigenstates $\psi_n(\vec{r}, t)$ form a complete basis of states.

The electromagnetic wave Equation 3.3 can be written in the same form as the TISE if we consider solutions of the form $\vec{E}(\vec{r}, t) = \vec{E}_\omega(\vec{r})\exp(-i\omega t)$, and limit ourselves to one specific component of the electric or magnetic field, say E_z. However, a complication arises when solving this problem. The curl operator is not Hermitian when the dielectric permittivity function $\varepsilon(\vec{r})$ varies from place to place, so the electric field must be properly rescaled. We instead consider solutions of the form $\vec{\phi}_w(\vec{r}) = \sqrt{\varepsilon(\vec{r})}\vec{E}_w(\vec{r})$. Plugging this into the electromagnetic wave Equation 3.2 we find:

$$\frac{1}{\sqrt{\varepsilon(\vec{r})}}\nabla \times \left[\nabla \times \frac{\vec{\phi}_w(\vec{r})}{\sqrt{\varepsilon(\vec{r})}}\right] = \frac{\omega^2}{c^2}\vec{\phi}_w(\vec{r}) \tag{3.6}$$

These eigenstates $\vec{\phi}_w(\vec{r})$ also form a complete basis of states, and we arrive at a new orthogonality relationship for the electric field:

$$\int d\vec{r}\vec{\phi}_m(\vec{r})\vec{\phi}_n(\vec{r}) = \int d\vec{r}\varepsilon(\vec{r})\vec{E}_m(\vec{r})\vec{E}_n(\vec{r}) = \delta_{mn} \tag{3.7}$$

If we apply the same vector identity as before, $\nabla \times (\nabla \times \vec{K}) = \nabla(\nabla \cdot \vec{K}) - \nabla^2\vec{K}$, and remember that $\nabla \cdot \vec{E} = 0$, we arrive at an electromagnetic wave equation of the same form as the TISE.

$$\left[\nabla^2 - \frac{\omega^2}{c^2}(1 - \varepsilon(\vec{r})) + \frac{\omega^2}{c^2})\right]\vec{E}_w(\vec{r}) = 0 \tag{3.8}$$

As can be seen, Equations 3.5 and 3.8 have an identical structure. By setting $\varepsilon(\vec{r}) = 1$ and the potential $V(\vec{r}) = 0$, one can find the constant $E_{light} = \frac{(\hbar\omega)^2}{2mc^2}$ which can be used to relate the quantum mechanical potential in the TISE to the dielectric permittivity in the EM wave equation $V(\vec{r}) = E_{light}(1 - \varepsilon(\vec{r}))$. Both equations support plane-wave solutions of the form $\psi_E(\vec{r}) = \psi_w(\vec{r}) = \psi_{k,w} exp(i\vec{k} \cdot \vec{r} - i\omega t)$, where the wave-vector $\vec{k}$ is related to the frequency ω by $\|\vec{k}\| = k = \omega\sqrt{\varepsilon\varepsilon_0\mu_0} = \frac{n\omega}{c}$ and n is the index of refraction.

3.3. DISCRETIZATION OF THE WAVE EQUATION

In the previous sections we explored how Schrodinger's wave equation is identical in structure to the electromagnetic wave equation. However, before we move on, we must briefly discuss some minor considerations one must deal with when these equations are discretized and solved with a computer. This changes how some of the variables relate to one another, so we will now workout the exact relationship between grid size, permetivitty, potential, energy, etc., under these new conditions.

We want to solve the Maxwell's equation in 2D for the tranverse modes,

$$\left[\nabla^2 + k^2\varepsilon(x, y)\right] E_z(x, y) = 0, \tag{3.9}$$

where $k = w/c$ is the frequency. When discretized (with central difference) on a square lattice with grid size Δh, this becomes

$$\frac{1}{\Delta h^2}\left(\psi_{i+1,j} + \psi_{i-1,j} + \psi_{i,j+1} + \psi_{i,j-1} - 4\psi_{i,j}\right) + k^2\varepsilon_{i,j}\psi_{i,j} = 0, \tag{3.10}$$

where $\psi_{i,j} = E_z(i\Delta h, j\Delta h), \varepsilon_{i,j} = \varepsilon(i\Delta h, j\Delta h)$.

In comparison, KWANT solves the Anderson model, which on a 2D square lattice is

$$t\left(\psi_{i+1,j} + \psi_{i-1,j} + \psi_{i,j+1} + \psi_{i,j-1}\right) + V_{i,j}\psi_{i,j} = E\psi_{i,j}, \tag{3.11}$$

where t is the hopping rate, $V_{i,j}$ is the on-site potential, and E is the energy.

We see that Equation 3.10 and Equation 3.11 are equivalent if we make the change of variables such that

$$(k\Delta h)^2 \varepsilon_{i,j} - 4 = \frac{1}{t}\left(V_{i,j} - E\right). \tag{3.12}$$

There are multiple ways to satisfy Equation 3.12. For simplicity, here we impose that in the free space (both on the left and on the right of the scattering region), $V_{i,j} = 0$ and $\varepsilon_{i,j} = 1$. Then we have

$$\begin{aligned} (k\Delta h)^2 &= 4 - E/t \\ \varepsilon_{i,j} &= 1 + \frac{V_{i,j}/t}{4 - E/t} \end{aligned} \tag{3.13}$$

In particular, if $V_{i,j} = d \cdot f_{i,j}$ where $-1 < f < 1$ is a random variable with zero mean, then $\varepsilon_{i,j} = 1 + \epsilon_{sca} f_{sca}$ with $\epsilon_{sca} = (d/t)(4 - E/t)$.

4. A COMPUTATIONAL EXPERIMENT WITH A DISORDERED DIELECTRIC WAVEGUIDE

The primary emphasis of this project is to compute an optimal wave-front which will maximize the transmission through a randomly disordered dielectric medium. With this goal in mind, we'll begin by briefly discussing the KWANT system itself, which was the computational library used to do the scattering matrix computations, and then we will give a brief description of the system we simulated within KWANT; this will also include a description of KWANT's basis functions and their average transmission since this will be important to understanding our final results. Next we will discuss eigenchannels, which are optimal wave-front solutions for individual disordered systems that can exhibit nearly 100% transmission. Then we explore a procedure to optimize the average transmission of a computed wave-front for a large number of randomly disordered systems. This method will utilize a transformation matrix to perform a change of basis, and then we will optimize the average transmission of these basis functions throughout all systems in the ensemble. Finally we will discuss the results obtained.

4.1. KWANT SIMULATION PACKAGE

KWANT is a free, open source Python package, focusing on numerical calculations of tight-binding models, particularly for quantum transport. It is frequently used to simulate metals, graphene, topological insulators, with the goal of studying phenomena such as the quantum Hall effect, superconductivity, spintronics, molecular electronics, and many others. KWANT was developed by an international community of scientists, receiving funding from many international scientific organizations including the US Office of Naval Research, the European Research Council, the Netherlands Organisation for Scientific Research NWO (formerly NWO/FOM), the French National Agency for Research (ANR), and many others.

4.2. DESCRIPTION OF THE SYSTEM

The first system we will be working with is not unlike that discussed in the scattering matrix formalism. It is illustrated in Figure 4.1.

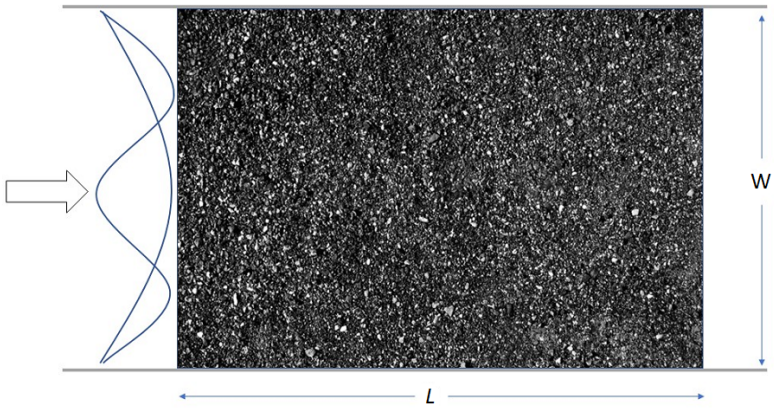

Figure 4.1. A Disordered Dielectric Slab. We used $L = 1000, W = 300$.

As one can see, this dielectric slab is contained within a waveguide. In the introduction, the modes of a waveguide were worked out, and as one might expect, the KWANT solutions can be resolved into a sum of waveguide modes. In this new case, the dielectric medium is 2D, defined in the x, y plane; the x-axis is the long axis of the waveguide and is the direction of wave propagation, the y-axis is the shorter aspect of the waveguide, and the z-axis comes up out of the page; we are examining the E_z component. Our solutions are of the general form

$$\begin{aligned} X_n(y) &= \sqrt{\frac{2}{W}} \sin(n\pi y/W) \\ \psi_\omega(x) &= \sum_{n=1}^{N} \left[C^+_{\alpha,n} X_n(y) \frac{e^{ik_n^{(x)}x}}{\sqrt{k_n^{(x)}}} + C^-_{\alpha,n} X_n(y) \frac{e^{-ik_n^{(x)}x}}{\sqrt{k_n^{(x)}}} \right] \end{aligned} \tag{4.1}$$

$$\begin{aligned} N &= \frac{\omega W}{c\pi} \\ k_n^{(x)} &= \sqrt{\frac{\omega^2}{c^2} - (n\pi/W)^2}, \end{aligned} \tag{4.2}$$

where $C^{+}_{\alpha,n}$ denotes the amplitude of the right moving waves and $C^{-}_{\alpha,n}$ denotes the amplitude of the left moving waves. $X_n(y)$ is the transverse mode profiles, similar to Equation 2.4.

This system was defined in KWANT, and the the slab itself was divided into a grid of integer step-size $\triangle h = 1$; a random potential was assigned to each point according to the formula $V = d \cdot random(-1, 1)$, where $d = 0.44$ and $random(-1, 1)$ is a function which returns a value between -1 and 1. An ensemble of systems of this type were generated, each filled with this disordered potential; the system parameters were carefully selected in order to ensure that we remained within the optical diffusive regime, a domain where photons travel through the material without being absorbed, instead undergoing repeated scattering events which change their path direction. The d value in particular was chosen so that within our ensemble of systems, each system's dimensionless conductance had a $g \approx 6-7$, where $g = (\pi/2)\, N \dfrac{l}{L}$ and l is the transport mean free path. The dimensions of the waveguide were $W = 300, L = 1000$ and the number of modes chosen was $N \approx 100$, where $N \approx \dfrac{1}{\pi} kW$, and we specifically chose $k = 1$. For the diffusive regime, we desire $kl \gg 1$, $N \gg 1$, $l \ll L$, and $g \gg 1$. In our case, $kL \approx 1000 \gg 1$, and $l \approx 41 \triangle h \ll L = 1000$, clearing satisfying all the conditions discussed above. KWANT computed the scattering matrices for each individual system and transmission was analyzed.

Let us briefly take a look at some of these basis functions and how they were indexed. For this dielectric slab system, KWANT used $N = 99$ different basis functions, indexed $0 - 98$, each of which were real valued $X_n(y)$ waves of varying spatial frequency. The real-part of the function is illustrated in blue and the imaginary part in orange in Figure 4.2. As one decreases in the index n, the spatial frequency increases, eventually becoming so large that that the spatial discretization is not adequate, leading to what appears to be an sine outer-envelope, but this is simply an artifact of finite discretization.

4.3. NUMERICAL ANALYSIS OF THE TRANSMISSION MATRICES

The scattering matrices for 2,000 different randomly disordered slabs were computed, and the transmission matrices t_{mn} were recorded. The absolute magnitude squared of each matrix element $T_{mn} = |t_{mn}|^2$ was taken, and then an average, denoted as $\langle ... \rangle$, was computed over all 2,000 of the systems. $\langle T_{mn} \rangle$ is illustrated in Figure 4.3.

As was discussed in the scattering matrix formalism, the sum of the n'th column of this matrix is the transmission of channel n. Just so that we don't get lost in the formalism and jargon, we're talking about the the total average wave flux transmission of each individual KWANT basis wave-front $X_m(y)$ through the different slabs. Figure 4.3 shows how $X_n(y)$ is transmitted into $X_m(y)$ to the right. The highest transmission coefficient $\langle T_{mn} \rangle$ is from $n = 1$ into $m = 1$ and the lowest is from $n = N$ into $m = N$. Transmission of each channel is illustrated in the next plot in Figure 4.4a, while a rescaled display of the same results is found in Figure 4.4b, where the red-dotted line, $\rho(\mu) = \mu + \triangle_b$, with $\triangle_b = 0.818$, is the predicted results from Radiative Transfer Theory (RTT) (Yamilov, 2008).

As one can see, on average, less than 10% of the wave flux is transmitted through to the other side of the slab, regardless of the $X_n(y)$ function used, and this transmission greatly decreases for high spatial frequencies. Remember, the lower the index (equal to $N - n$), the *higher* the spatial frequency. This is counter intuitive, but it is how KWANT indexes its basis functions.

4.4. EIGENCHANNELS: OPTIMAL WAVEFRONTS FOR A SINGLE SYSTEM

As indicated in the scattering formalism, if we know the scattering matrix for a given system, for any arbitrary impinging wavefront we can compute the waveform that will be transmitted along with its total wave-flux transmission. What if we wished to mathematically

compute the optimal wave-front which would have *maximal* transmission? How would we go about this? This can be done by performing a singular value decomposition on the transmission matrix.

To begin, we recall that the input and output waveforms are related by the scattering matrix, though if one desires, one can focus solely on the transmission by focusing attention on the transmission submatrix alone.

$$\vec{C}_r^+ = \hat{t}\vec{C}_l^+ \tag{4.3}$$

Next we perform a singular value decomposition on the transmission matrix.

$$\vec{C}_r^+ = \hat{U}\hat{\tau}^{\frac{1}{2}}\hat{V}^\dagger\vec{C}_l^+ \tag{4.4}$$

The matrices $\hat{U}$ and $\hat{V}$ are both unitary matrices whose values are complex. The matrix $\hat{\tau}$ is a rectangular diagonal matrix whose entries are real and non-negative, and are referred to in mathematics as the singular values of the transmission matrix. This means that these diagonal entries are the square-roots of the eigenvalues of $\hat{t}^\dagger\hat{t}$ or $\hat{t}\hat{t}^\dagger$. That's why this matrix is written as $\hat{\tau}^{\frac{1}{2}}$ and not just $\hat{\tau}$.

Now if one uses the i'th column of $\hat{V}$ for the input $\vec{C}_l^+$, this excites what is called the i'th "eigenchannel" of the system. But why are these particular waveform inputs so special? First note that $\hat{V}^\dagger\hat{V} = \hat{I}$, where $\hat{I}$ is the identity matrix. Let us consider what happens if we multiply $\hat{V}^\dagger$ by a vector consisting of a column of $\hat{V}$. We will get the following,

$$\hat{V}^{\dagger}\begin{bmatrix} i'th \\ column \\ of \\ \hat{V} \end{bmatrix} = \begin{bmatrix} 0 \\ \vdots \\ 0 \\ 1 \\ 0 \\ \vdots \\ 0 \end{bmatrix}, \tag{4.5}$$

where the 1 will be located in the i'th index of the column vector. So let's apply this technique to our system.

$$\vec{C}_r^{+} = \hat{U}\begin{bmatrix} \tau_1^{1/2} & & \\ & \ddots & \\ & & \tau_n^{1/2} \end{bmatrix}\hat{V}^{\dagger}\begin{bmatrix} i'th \\ column \\ of \\ \hat{V} \end{bmatrix} \tag{4.6}$$

Now this further simplifies to the following

$$\vec{C}_r^{+} = \hat{U}\begin{bmatrix} \tau_1^{1/2} & & \\ & \ddots & \\ & & \tau_n^{1/2} \end{bmatrix}\begin{bmatrix} 0 \\ \vdots \\ 0 \\ 1 \\ 0 \\ \vdots \\ 0 \end{bmatrix} \tag{4.7}$$

Taking this one step further, it becomes quite clear why this important.

$$\vec{C}_r^{+} = \hat{U} \begin{bmatrix} 0 \\ \vdots \\ 0 \\ \tau_i^{1/2} \\ 0 \\ \vdots \\ 0 \end{bmatrix} \tag{4.8}$$

If we now square $\vec{C}_r^{+}$ we come to most revealing step.

$$|\vec{C}_r^{+}|^2 = \vec{C}_r^{+\dagger}\vec{C}_r^{+} = \begin{bmatrix} 0 \dots \tau_i^{1/2} \dots 0 \end{bmatrix} \hat{U}^{\dagger}\hat{U} \begin{bmatrix} 0 \\ \vdots \\ \tau_i^{1/2} \\ \vdots \\ 0 \end{bmatrix} = \tau_i \tag{4.9}$$

Let us analyze our result. In short, for the i'th eigenchannel, $\tau_i \cdot 100\%$ is the channel's percentage of wave-flux transmission. The i'th column of the $\hat{U}$ matrix tells us how this wave-flux is distributed to the different components of the output vector, but the total transmission is $\tau_i \cdot 100\%$. As stated before, these τ_i values are always real, positive, and less than or equal to 1. The typical values of τ_i are illustrated in Figure 4.5. As can be seen in Figure 4.5b, the average transmission for the n'th eigenchannel follows a $\tau_i \approx 1/\cosh^2(C \cdot (g/N) \cdot i)$ curve, which is standard throughout optical and quantum transport literature (Davy *et al.*, 2015; Yuli V. Nazarov, 2009).

In practice, when using various computational matrix libraries to perform the singular value decomposition, the τ_i values are arranged in descending order. So the early τ_i values, such as τ_1, τ_2, τ_3, etc., will be very close to 1, if not 1 exactly. This means that if you stimulate the early eigenchannels, you will get nearly, if not perfect, 100% transmission.

But remember, as one moves down the list, the τ_i values decrease, and toward the end can get close to 0, meaning they have very poor transmission. For this reason, the early, highly transmitting eigenchannels are called “open", and the later, low transmitting eigenchannels are called “closed".

So what do these eigenchannel wavevectors look like? Do you they have some sort of easily identifiable pattern? For example, say we take 500 different randomly generated dielectric slab systems, and we compute the first eigenchannel for each system. If we were to place all of these waveforms side by side, would we notice any similarities? Let’s do that and see. We’ll create a heatmap where the entries of each column represents the square magnitudes of the vector components of the first eignenchannel. In other words, all of the column entries are the contributions of the different $X_n(y)$ basis waves for each eigenchannel. Let’s take a look.

From a cursory look at Figure 4.6, it doesn’t look like there’s any sort of simple pattern to the highly transmitting eigenchannels. The systems are random and it looks like the top eigenchannel for each system is just as random. Maybe it wouldn’t hurt to also look at the next eigenchannel in just the same way?

Once again, there is no obvious pattern. From Figure 4.6 and Figure 4.7, it looks like the highly transmitting eigenchannels are different for each system. So, if we are hoping to create a highly transmitting wavefront which will transmit through all 500 systems in our ensemble with nearly perfect transmission, it appears that we’re probably out of luck. Each system seems to need its own custom tailored wavefront to get nearly perfect transmission. However, maybe there is a wavefront which is still better than randomly exciting the system? Maybe there is some strange shaped wavefront that could still give us something like an average of 10% transmission across all systems? But if such a wavefront exists, how could one go about computing it? Also, would it have anything to do with the all of these systems’ eigenchannels? These are the questions we will attempt to address in the following section.

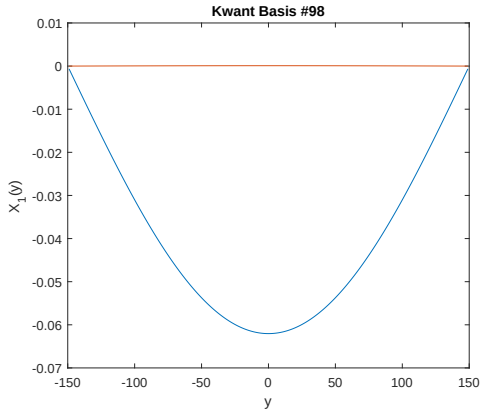

(a) KWANT Basis Wavefront 98
$n = N - 98 = 1$

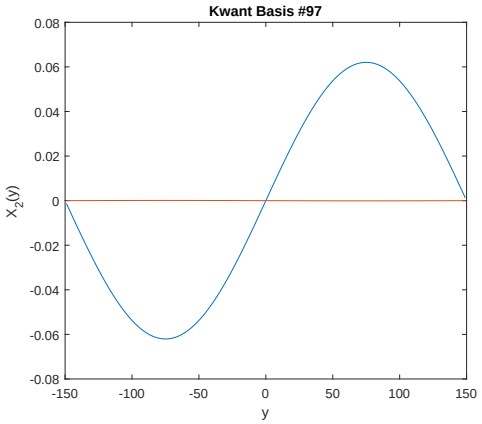

(b) KWANT Basis Wavefront 97
$n = N - 97 = 2$

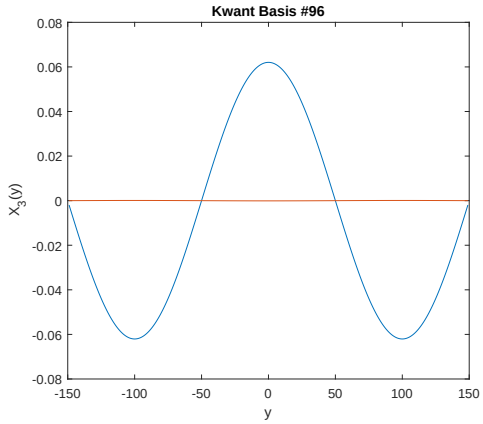

(c) KWANT Basis Wavefront 96
$n = N - 96 = 3$

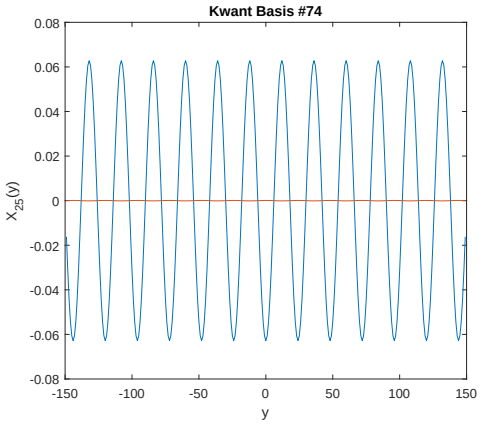

(d) KWANT Basis Wavefront 74
$n = N - 74 = 25$

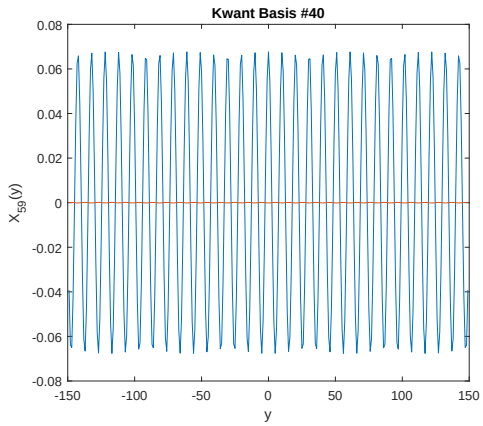

(e) KWANT Basis Wavefront 40
$n = N - 40 = 59$

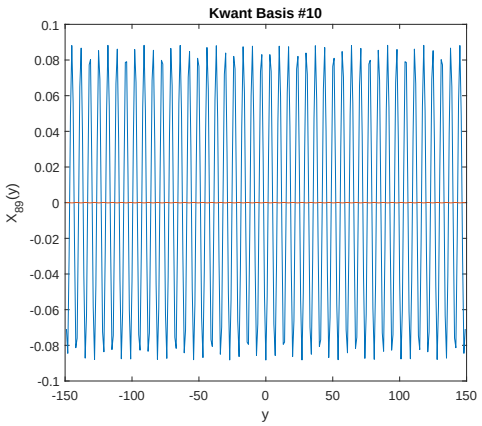

(f) KWANT Basis Wavefront 10
$n = N - 10 = 89$

Figure 4.2. KWANT Basis Functions. Notice that higher spatial frequency is with lower indices, not higher indices, this being a convention in the KWANT package.

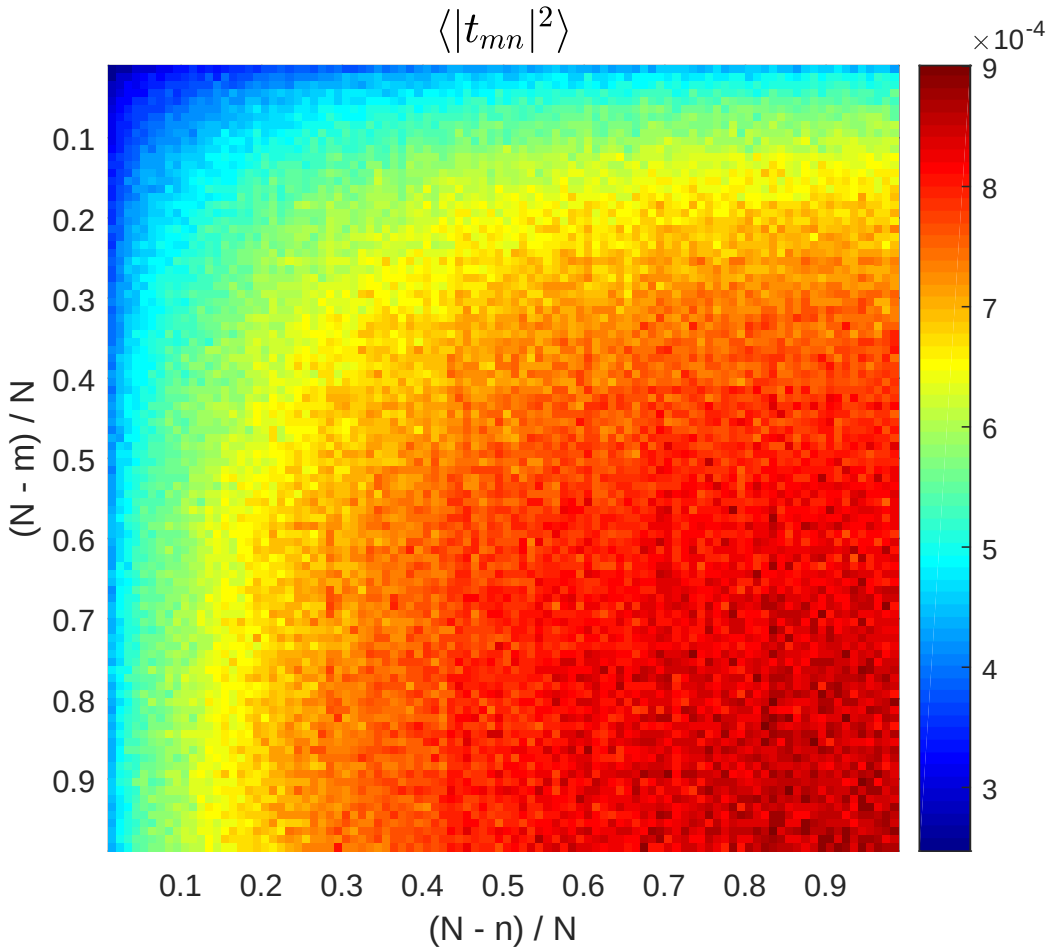

Figure 4.3. Transmission matrix $\langle |t_{mn}|^2 \rangle$ averaged over 2,000 realizations.

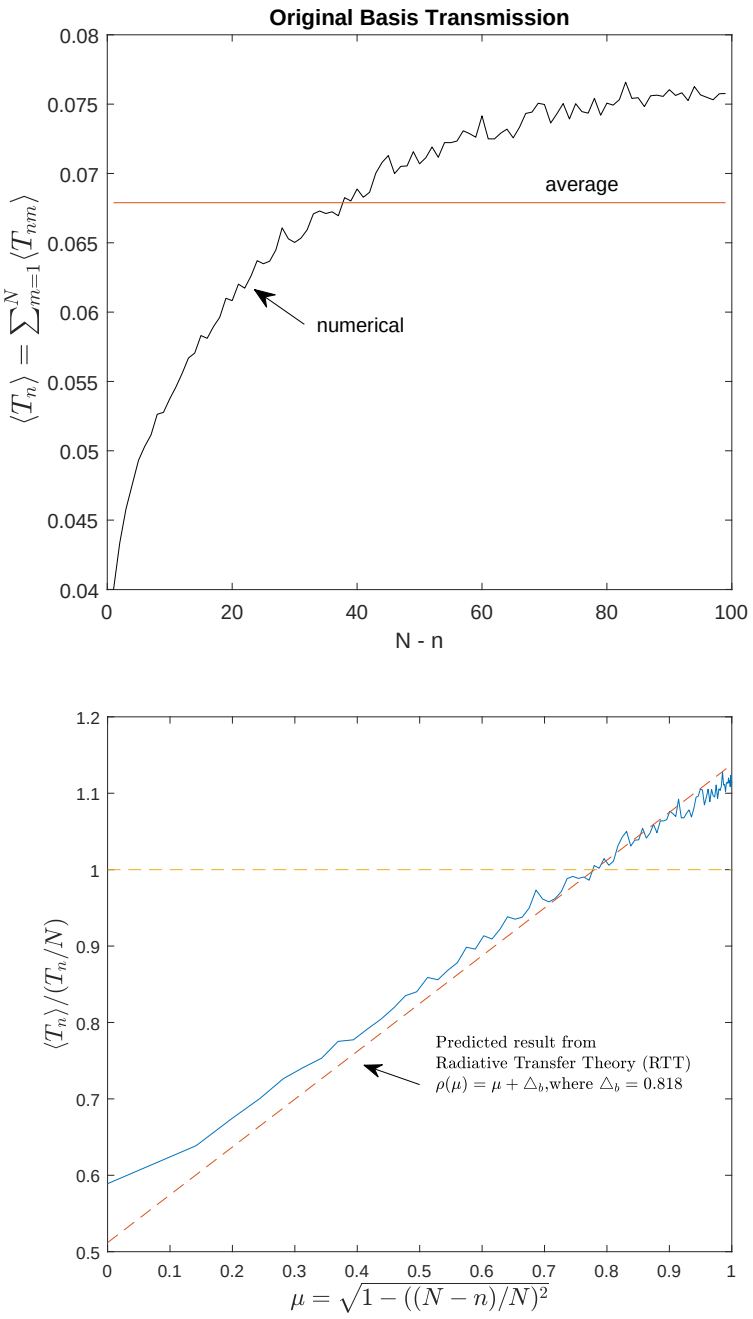

Figure 4.4. The average transmission of each of KWANT's basis wave-fronts over 2,000 realizations.

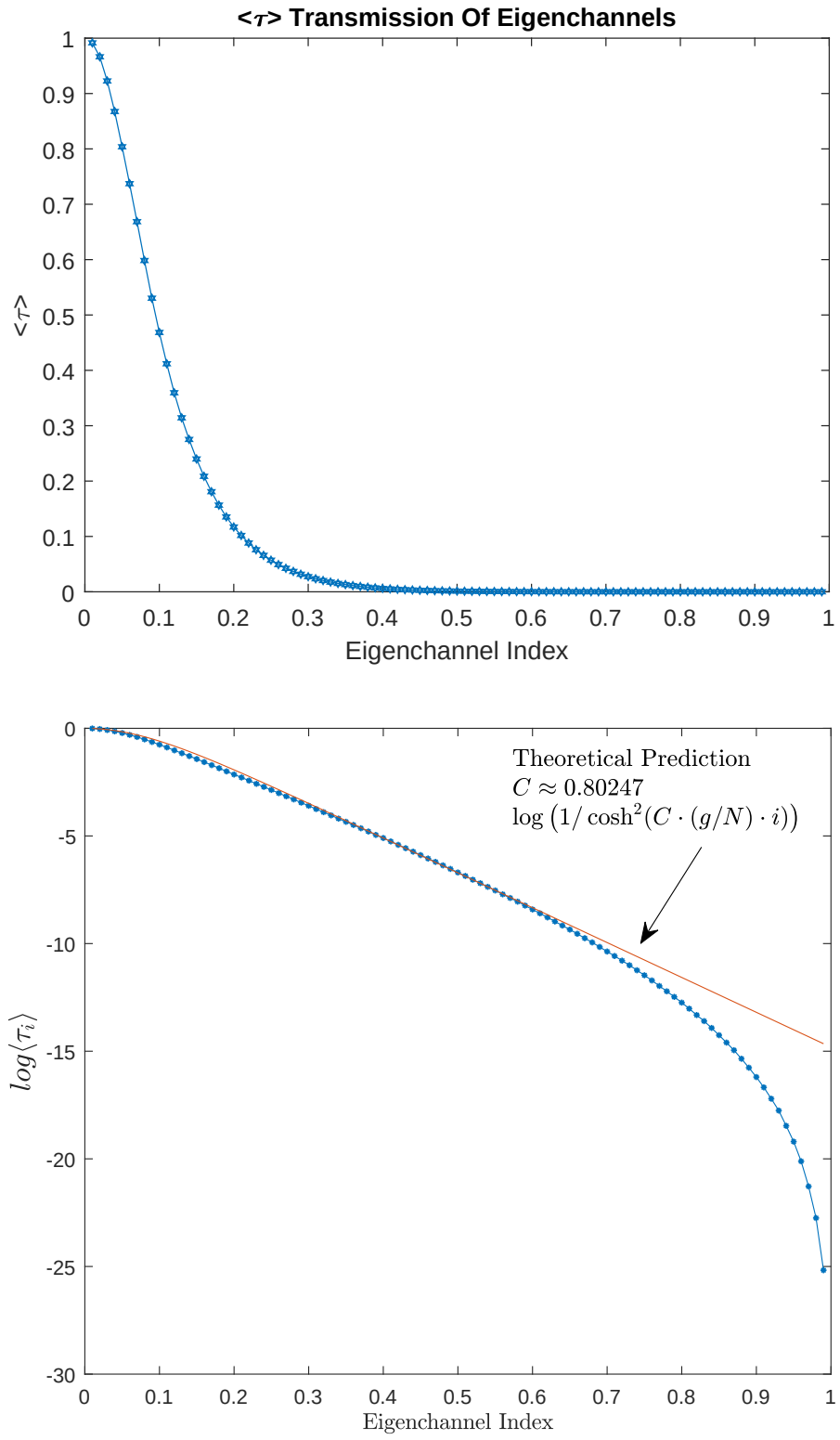

Figure 4.5. τ Values For Different Eigenchannels. The fact that there always exists a $\tau_i \approx 1$ is a highly non-trivial fact. It represents one of the most important discoveries in mesoscopic physics (Yuli V. Nazarov, 2009).

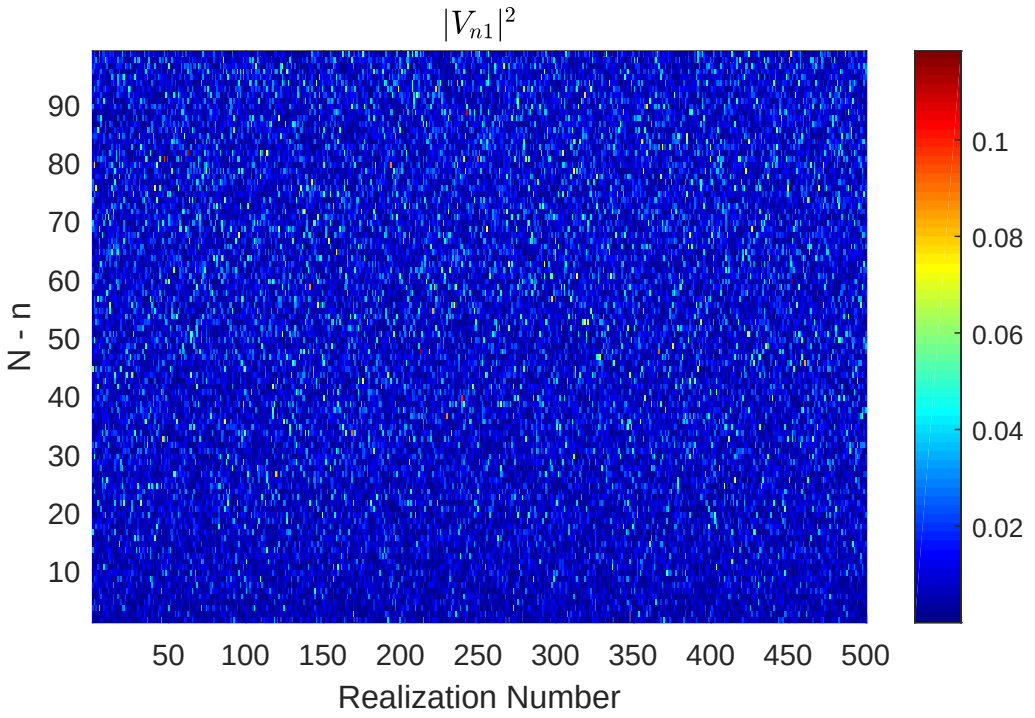

Figure 4.6. A look at the first eigenchannel for different systems side by side. V_{n1} are excitation amplitudes for $i = 1$ eigenchannel with $\tau_1 \approx 1$.

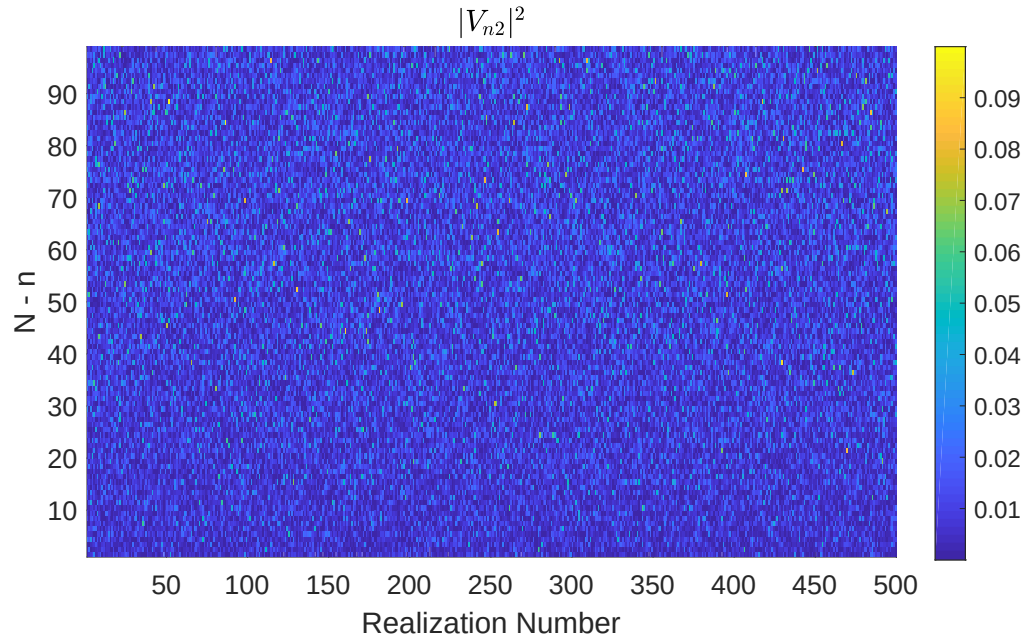

Figure 4.7. A look at the second eigenchannel for different systems side by side. V_{n2} are excitation amplitudes for $i = 2$ eigenchannel with $\tau_2 \approx 0.94$.

5. FINDING THE UNIVERSAL OPTIMAL WAVEFRONT

The real question we'd like to explore in this section is whether or not there is some complicated, special universal wavefront which gives a substantial enhancement of transmission no matter which system we try to send it through. Assume we know nothing about the system we're dealing with; is there some special wavefront which will always be our best bet? Mathematically speaking, we're asking for a wavefront that would have the highest average transmission, after attempting to send it through an extremely large collection of uncorrelated disordered systems. Considering what we saw with the top eigenchannels for each system, it was hard to see a pattern, but we will let a computer algorithm uncover potential patterns.

5.1. A HINT: AVERAGE OVER ALL TOP EIGENCHANNELS

Before we resort to an algorithmic approach to this problem, let us think about all we have learned so far in the previous sections and make an educated guess. For each system individually, there are a handful of top eigenchannels which individually give nearly perfect transmission. So if we're sending a wavefront through an ensemble of $2,000$ different random systems, what if we just averaged the top eigenchannels and used that as our input vector? The question is, since these top eigenchannels were so random looking, will we see any pattern? Let's take a look! We know that the eigenchannels are simply the columns of the $\hat{V}$ matrix, so let's compute $\langle|\hat{V_{ni}}|^2\rangle$, the average $|\hat{V_{ni}}|^2$ over $2,000$ different randomly disordered systems. The i'th column of this picture will be the averaged i'th eigenchannel over $2,000$ different systems. What is Figure 5.1 telling us?

5.1.1. A Look At The Worst Transmitting Averaged Eigenchannels. If we look at $\langle|V_{ni}|^2\rangle$, the worst transmitting eigenchannels, particularly columns $i = 85 - 98 \approx N$, we see a large amplitude spot in the top-right corner. This represents very large contributions

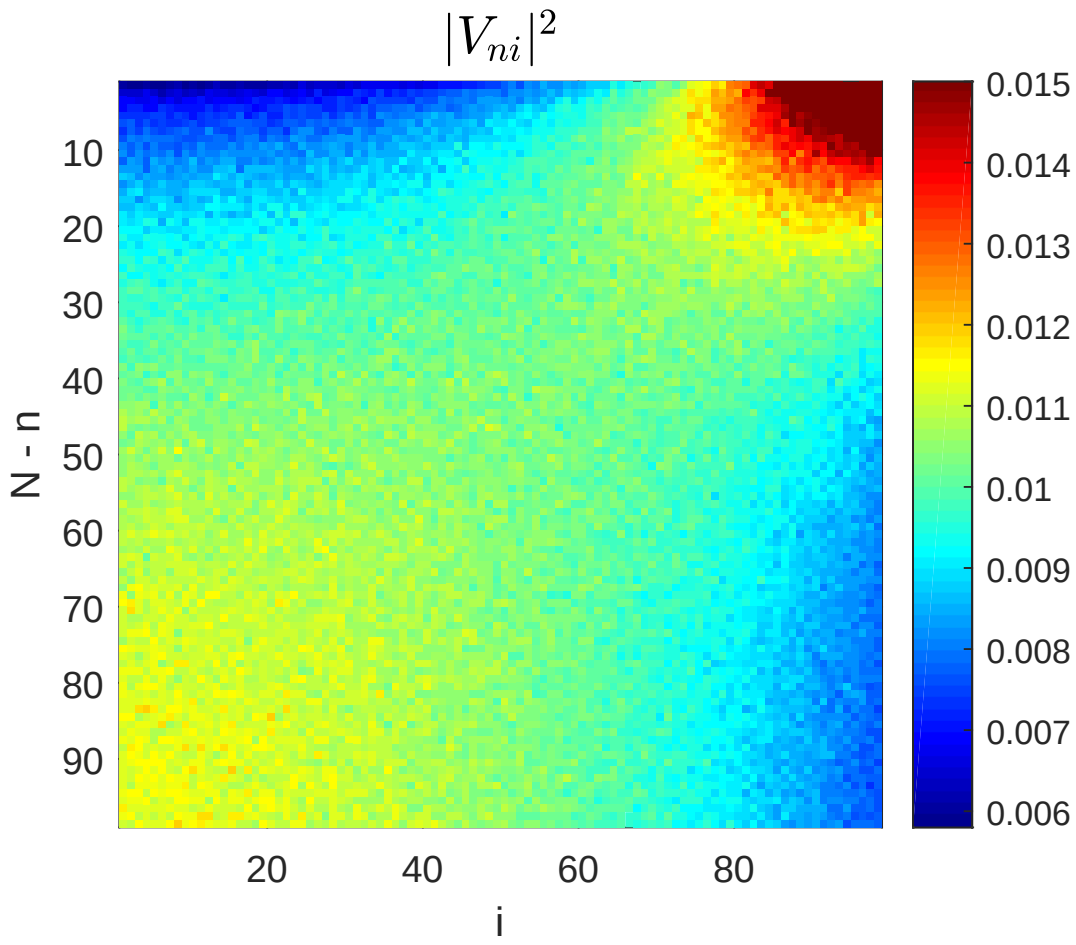

Figure 5.1. $\langle |V_{ni}|^2 \rangle$ Averaged Over 2000 Realizations.

from the first ten or so basis functions $X_n(y)$ with $n \approx N$. Now refer back to Figure 4.4, where we saw the average transmission of the KWANT basis functions over thousands of realizations. These basis functions with the highest spatial frequency, had with the worst average transmission of all the basis functions. So the worst average eigenchannels utilize components which have the worst average transmission. Makes sense.

5.1.2. A Look At The Best Transmitting Averaged Eigenchannels. Now let's examine the best transmitting averaged eigenchannels, specifically columns $i = 0 - 10$ of Figure 5.1; we see a dark spot in the top-left corner, meaning eigenchannels with the highest transmission avoid these high spatial frequency, low transmitting basis functions. So a pattern emerges. However, it's not so clear that there's any other pattern, at least at a glance.

The most we can say is they avoid high spatial frequency basis functions, and seem to use contributions from the other basis functions, particularly $n \approx 1 - N/2$, relatively equally. Still, there might likely be another pattern. If the best averaged eigenchannels are avoiding the basis functions with low average transmission, it's likely that they're going to have high contributions from the basis functions with the highest average transmission. But if that were the case, wouldn't we see another bright spot at the bottom-left corner of Figure 5.1? No, not actually. While basis function 98 ($n = 1$) has the highest average transmission, it doesn't differ all that much from basis functions $60 - 97$. Their average transmission ranges from 0.072 to 0.076, which is only a 5.3% difference overall. Compare this to the first 10 or so basis functions, which have average transmissions in the range of 0.040 to 0.055, which is a much greater percent difference. It's not surprising that the top average eigenchannels would utilize all the best transmitting basis components, which can come from any of the $60 - 98$ range, considering their overall average transmission is nearly the same. Also, another hint, note that the higher transmitting eigenchannels are utilizing components with lower spatial frequency.

5.2. A THOUGHT EXPERIMENT

To appreciate the above results, let's propose a simple thought experiment. To devise a simple, iterative computational algorithm to find a wavefront with optimal transmission through a very large number of randomly disordered systems, we begin with a random input wavevector and just keep making small random variations to the basis weights; with each tiny change, reevaluate the average wave-flux transmission, and check whether or not that change increased the transmission. If that change increased transmission, we keep it, if it did not, we discard it. (Note: we'd also have to make sure your weights were properly normalized too. After all, it wouldn't make sense if transmission exceeded 100%!) What would such an algorithm converge to? Since each system is random, would there any room for optimization at all? For an individual system, as one would probably guess, it would

eventually find an input vector which is a linear combination of the most highly transmitting eigenchannels, leaving it with nearly perfect transmission. But what if we're averaging over 500 or even 10,000 different systems? Will this algorithm find anything? Would there be some complicated wavefront which will find its way through all systems with an appreciable enhancement in transmission? This simple thought experiment gives the general idea of what we'll be doing with our algorithm, but our approach is a bit more sophisticated, and it will require bit more mathematics to prepare us for the final algorithm to be used. We will now go over this additional mathematics in the following subsection.

5.3. SOME MATHEMATICAL FORMALISM NEEDED TO COMPUTE THE UNIVERSAL WAVEFRONT

The goal of this section is to devise a computational algorithm which will give us an incoming wavefront with optimal transmission through a system, or collection of systems. We will accomplish this by first transforming the original basis functions (the $X_n(y) = \sqrt{\frac{2}{W}}\sin(n\pi y/W)$ waves) into some other form using a unitary transformation matrix. After this transformation is complete, we will then reevaluate the transmission of each new transformed basis function and compute a "cost" function which will be a weighted sum of the average transmission of the new basis functions throughout all systems being considered. We will then optimize this cost function, and the first basis function in this new transformed basis will have the highest transmission.

We begin by transforming the transmission matrix using a unitary transformation matrix $\hat{A}$.

$$\begin{aligned} \hat{A}^\dagger \hat{A} = \hat{A}\hat{A}^\dagger = \hat{I} \\ \hat{\tilde{t}} = \hat{A}\hat{t}\hat{A}^\dagger \\ \vec{\tilde{C}} = \hat{A}\vec{C} \\ \vec{\tilde{C}}_r^+ = \hat{\tilde{t}}\vec{\tilde{C}}_l^+ \end{aligned} \tag{5.1}$$

In this notation, the tilde represents the transformed mathematical object. The matrix A must always remain unitary because, as noted prior, this unitarity represents a conservation of wave-flux. The original basis functions end up being transformed as follows.

$$\tilde{\psi}_i(\vec{r}) = \sum_{n=1}^{N} A_{in}\psi_n(\vec{r}) \tag{5.2}$$

Therefore, the newly transformed i'th basis function is a linear combination of the old basis functions, using the i'th row of $\hat{A}$ as the transformation weights. All wavefunctions are to be transformed in this way.

Now we must discuss transmission in this new basis, and how we will compute the cost function which we will be optimizing. The transmission of the new i'th basis function now becomes the sum of the squared magnitude of all the i'th column entries within the newly transformed transmission matrix.

$$\tilde{T}_i = \sum_{m=1}^{N} |\tilde{t}_{mi}|^2 \tag{5.3}$$

Our cost function is a weighted sum of the average transmission of all the new basis functions across all systems being considered.

$$\triangle = \sum_{n=1}^{N} \left(\frac{1}{n+1}\right) \langle \tilde{T}_n \rangle \tag{5.4}$$

As will be discussed in a moment, our algorithm will be randomly changing entries in the transformation matrix $\hat{A}$, and then reevaluating transmission, along with this particular cost function. In the following we motivate our specific choice of cost function and also discuss other potential approaches, such as a simultaneous optimization of all channels.

In the scattering matrix formalism, we went to great lengths to stress wave-flux conservation. This is just as important when we change to a new basis. The flux of an incoming wavefront must either be transmitted or reflected, in any basis. This is reflected

in the next equation.

$$T_n + R_n = \tilde{T}_n + \tilde{R}_n = 1 \tag{5.5}$$

for any n. So if we sum over all channels, we arrive at the following.

$$T + R = \sum_n^N (T_n + R_n) = \tilde{T} + \tilde{R} = \sum_n^N (\tilde{T}_n + \tilde{R}_n) = N \tag{5.6}$$

In other words, the sum of the total transmission and total reflection of all channels remains constant. We will now prove that the total transmission and total reflectance also individually remain constant.

$$\begin{gathered} Tr(\hat{t}^\dagger \hat{t}) = \sum_{ab} t_{ab}^* t_{ba} = \sum_{ab} |t_{ab}|^2 = T \\ Tr(\hat{\tilde{t}}^\dagger \hat{\tilde{t}}) = Tr(\hat{A}\hat{t}^\dagger \hat{A}^\dagger \hat{A}\hat{t}\hat{A}^\dagger) = Tr(\hat{A}\hat{t}^\dagger \hat{t}\hat{A}^\dagger) = Tr(\hat{A}\hat{A}^\dagger \hat{t}^\dagger \hat{t}) = Tr(\hat{t}^\dagger \hat{t}) = T \end{gathered} \tag{5.7}$$

Therefore, if we do a transformation which increases the transmission of one particular channel, it must be accompanied by a reduction in the transmission of the other(s). The same applies to reflectance. With this in mind, when we do a basis transformation to optimize the transmission of the first few new channels, we in turn decrease the transmission of the other channels. Considering that the total transmission available to all channels is T, our cost function is designed to maximize the transmission of the first few channels, at the expense of later channels.

5.4. THE ALGORITHM FOR COMPUTING AN OPTIMAL WAVEFRONT

In this section we will quickly outline of the actual algorithm used to compute an optimal wavefront with maximal transmission.

General Algorithm

Loop over each row of the transformation matrix $\hat{A}$, one at a time

Randomly select an entry $A_{ni} = a_{ni}e^{i\phi_{ni}}$ within the row

Make a slight modification to A_{ni} as follows:

$\Rightarrow$ *with probability 1/2:* $a_{ni} \rightarrow a_{ni} \cdot (1 + \delta)$

$\Rightarrow$ *with probability 1/2:* $\phi_{ni} \rightarrow \phi_{ni} + \delta \cdot \pi$

Make sure A remains unitary using the QR technique listed below

Recompute the "Cost" function

$\Rightarrow$ *If this change increases the "Cost" function, keep the change*

$\Rightarrow$ *If this change decreases the "Cost" function, discard it.*

Continue looping over all rows as long as the "Cost" function is increasing

---

As mentioned in the algorithm, the matrix $\hat{A}$ was kept unitary by using a QR factorization algorithm, listed below. This algorithm allows one to make changes to $\hat{A}$, yet still retain unitarity and the general structure of any changes made. This algorithm is listed as the actual Python code used.

Making Sure Transformation Matrix Remains Unitary

```
def makeMatrixUnitary(A)
  Q,R = np.linalg.qr(A)
  R = abs(np.diag(np.diag(R) / abs(np.diag(R))))
  return np.matmul(Q,R)
```

This algorithm was run so long as the “Cost" function was increasing. Once the algorithm converged very close to the maximal “Cost" value, we then saved the transformation matrix. We verified that this algorithm converged to the same unique (up to a constant phase factor) solution by doing multiple convergence runs.

5.5. RESULTS FOR A SINGLE SLAB SYSTEM

In this section we will go over the results the optimization algorithm found for the dielectric slab system within a waveguide (Figure 2.1). The convergence results are shown in Figure 5.2.

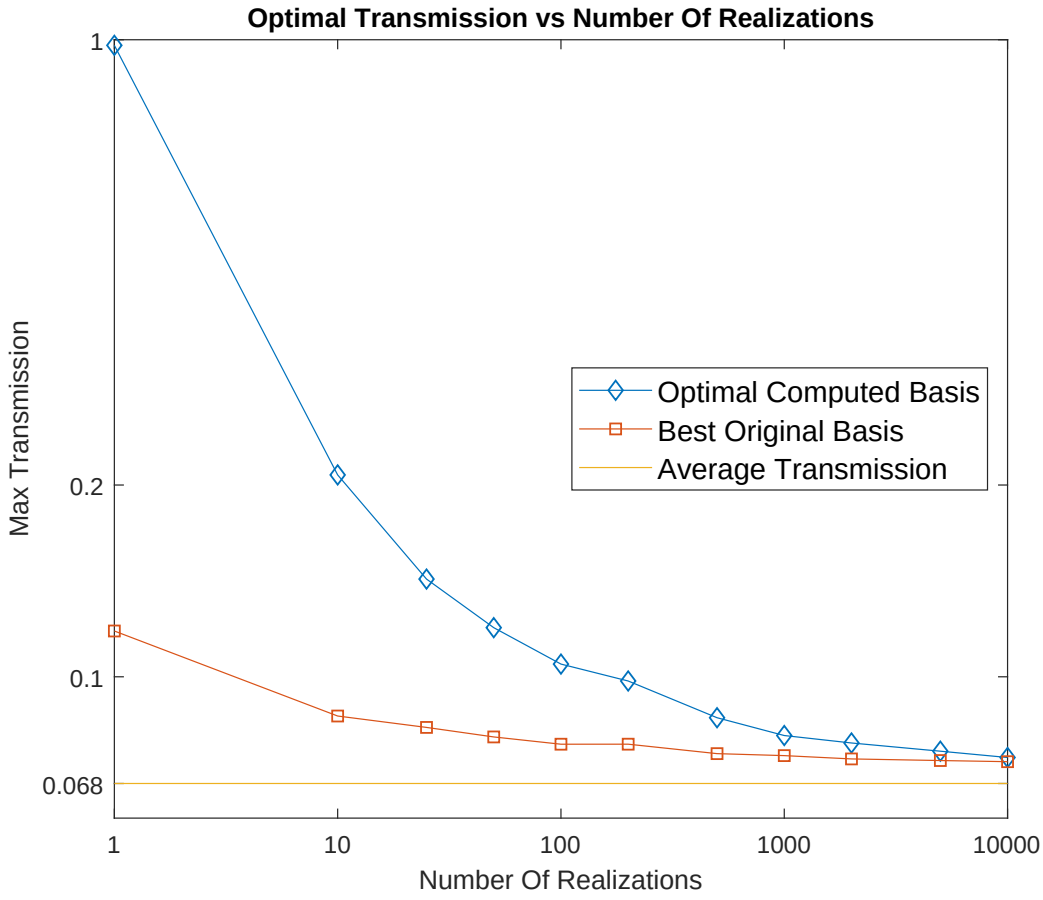

Figure 5.2. A comparison of maximal transmission. Blue symbols signify the best computed waveform transmission. Red symbols signify the best original basis function $X_1(y)$ transmission. In orange is the average transmission of all basis waveforms.

In this Figure, the bottom axis designates the number of randomly disordered systems that were averaged over and the vertical axis is the maximum transmission found. The blue symbols signify the average transmission of the best computed wavefront found by the algorithm, the red symbols are the average transmission of the best original basis function (in this case the $X_n(y)$ wave with longest wavelength, $X_1(y)$), and the orange line signifies the average of the average transmission of all basis functions combined, which never changes, even during our transformation. We observe that for a small number of systems, the algorithm can find some optimal wavefront which has much superior transmission. If you need to penetrate through five or ten systems, some complicated wavefront exists which will give you something like $20 - 50\%$ transmission, no problem. For a single system it can find nearly perfect transmission with $T_i = max[\tau_i] \approx 1$. However, as more and more systems are taken into account, the best wavefront's transmission decreases monotonously, but it remains bound from below. After averaging over thousands of different systems, the best wavefront possible, in the case of systems structured like that found in Figure 4.1, is a simple $X_1(y)$ wavefront with the longest wavelength ($n = 1$). The question remains, why is this the case? That is what we will discuss in the next section.

6. CONCLUSIONS

6.1. INTERPRETATION OF RESULTS

Here we would like to find an intuitive explanation as to why, when averaging over a very large number of different systems, the highest transmitting (on average) basis function converges to the $X_n(y)$ with the longest wavelength. This result was obtained in Figure 4.4 as well as Figure 5.2.

Any waveguide mode can semiclassically be represented as a superposition of two bouncing modes with the same $k_{\|}$ and opposite $\pm k_{\perp}$. Each of these plane waves has a propagation vector $\vec{k}$, which (in 2D) has two components, $k_{\perp}$ which is directed normal to the system, and $k_{\|}$ which is parallel to the system. This is illustrated in Figure 6.1.

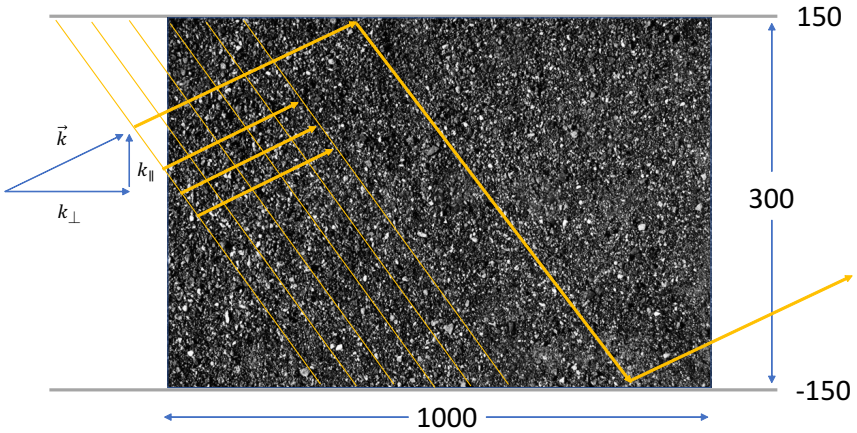

Figure 6.1. The $\vec{k}$ vector. Optimal average transmission occurs when $\vec{k}$ is directed nearly perpendicular to the surface.

We know that in the limit $k\Delta h \to 0$ that $k_{\perp} = \sqrt{k^2 - k_{\|}^2}$, and that $k_{\|}$ increases as one increases the spatial frequency of the parallel basis functions. We also know the maximum average transmission occurred every time we maximized $k_{\perp}$, hence also minimizing $k_{\|}$. So

it seems that in order to obtain the best transmission, we need to make sure our wavefront is incident near normal to the surface one is trying to transmit through, but what is special about normal incidence?

The central idea is that the highest transmitting path is the one with the least resistance; for the system we just considered, this path is where $\vec{k}$ is directly perpendicular to the surface. As a waveform makes its way through this disordered material, it is constantly being scattered, and the more scattering we have, the greater the chance that the wave flux will turn around and reflect instead of transmit. As one adds a parallel component to $\vec{k}$, we are taking a longer path through the disordered material and decreasing the average transmission. This is easily seen in Figure 6.1. So the key idea is not necessarily normal incidence, though in many systems this will be the case; it is about first identifying the path of least resistance for the particular system, and then directing maximium wave-flux intensity onto that path. We will further reinforce this conclusion in the next section.

6.2. IMPLICATIONS

Let's examine another system, illustrated in Figure 6.2, this time with a "hole" in the dielectric layer. What makes this system special is that "normal incidence" and "path of least resistance" routes are fundamentally different here. The random dielectric slab material was generated the same as before, only this time we leave an open hole from $y = -12$ to $y = 12$. If our former conclusion is correct, the path of least resistance will be to direct the wave flux through the "hole" in the material. Remember, our computational algorithm starts off completely random, with no preference for any wave-front in particular. After searching through countless wavefronts, the optimal solution found by the algorithm is illustrated in Figure 6.3. You can see that its intensity is all directed into the "hole", the path of least resistance. It is also instructive to look at the average waveform generated from this computed pulse wavefront, averaged over thousands of systems. This is illustrated in Figure 6.4. As the light propagates through the "hole", it generally stays within the crack

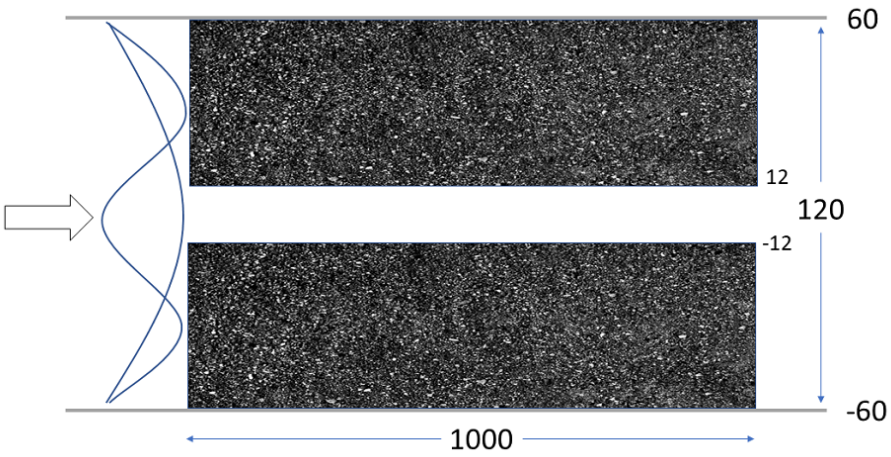

Figure 6.2. A dielectric slab with a hole in the center.

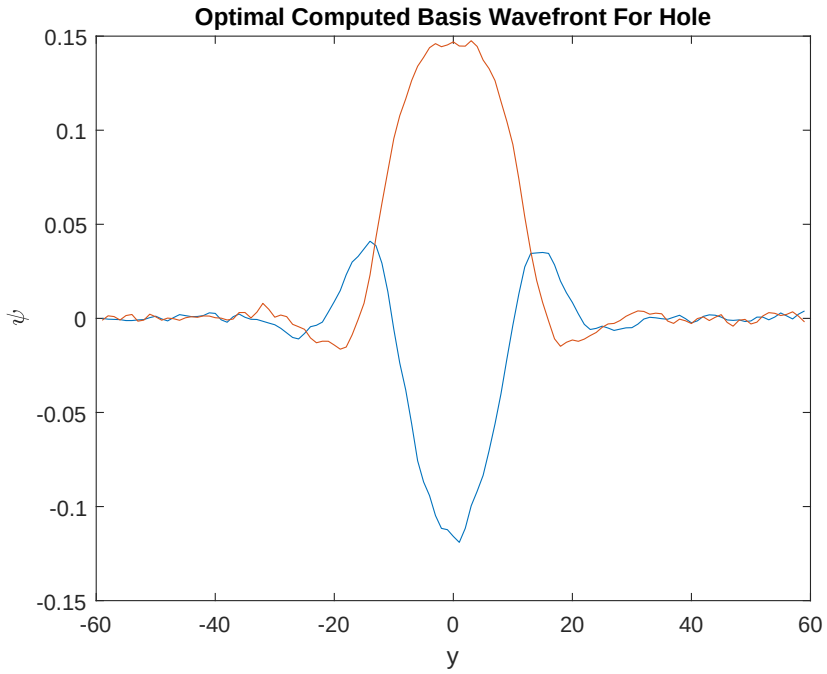

Figure 6.3. The Optimal Wavefront For Maximal Transmission Through The Hole.

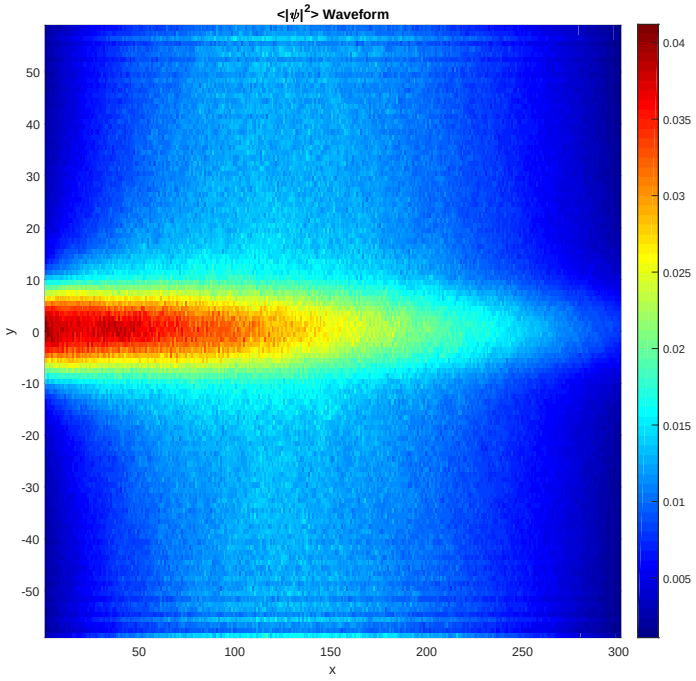

Figure 6.4. The Average Waveform Intensity Of The Computed Wavefront Pulse Through The Hole.

(the path of least resistance) but slowly diffuses into the surrounding material when coming into contact with the “hole" walls. One can easily imagine that this same idea could be applied to any sort of hole or crack. As a final remark we expect that this work will stimulate further effort to find “universal" (disorder-independent) wavefronts which can be used for more efficient transmission of waves through scattering media without sophisticated search of optimized wave fronts.

REFERENCES

Beenakker, C. W. J., 'Random-matrix theory of quantum transport,' Rev. Mod. Phys., 1997, **69**, pp. 731–808, doi:10.1103/RevModPhys.69.731.

Bekefi, G. and Barrett, A. H., *Electromagnetic Vibrations, Waves, and Radiation*, MIT Press, 1977, ISBN 9780262520478.

Davy, M., Shi, Z., Park, J., Tian, C., and Genack, A. Z., 'Universal structure of transmission eigenchannels inside opaque media,' Nature Communications, 2015, **6**, p. 6893.

Eric Akkermans, G. M., *Mesoscopic Physics of Electrons and Photons*, CAMBRIDGE UNIV PR, 2011, ISBN 0521349478.

Fink, M., 'Time reversed acoustics,' Physics Today, 1997, **50**(3), pp. 34–40, doi: 10.1063/1.881692.

Fink, M., Cassereau, D., Derode, A., Prada, C., Roux, P., Tanter, M., Thomas, J.-L., and Wu, F., 'Time-reversed acoustics,' Reports on Progress in Physics, 2000, **63**(12), p. 1933.

Freund, I., 'Looking through walls and around corners,' Physica A: Statistical Mechanics and its Applications, 1990, **168**(1), pp. 49–65, doi:10.1016/0378-4371(90)90357-X.

Goodman, J. W., *Speckle Phenomena in Optics*, W. H. Freeman, 2010, ISBN 1936221144.

Groth, C. W., Wimmer, M., Akhmerov, A. R., and Waintal, X., 'Kwant: a software package for quantum transport,' New Journal of Physics, 2014, **16**(6), p. 063065.

Kramer, *Quantum transport in semiconductor submicron structures*, Springer Netherlands, 1996, ISBN 0792341902.

Mosk, A. P., Lagendijk, A., Lerosey, G., and Fink, M., 'Controlling waves in space and time for imaging and focusing in complex media,' Nature Photonics, 2012, **6**, p. 283.

Popoff, S. M., Lerosey, G., Carminati, R., Fink, M., Boccara, A. C., and Gigan, S., 'Measuring the transmission matrix in optics: An approach to the study and control of light propagation in disordered media,' Phys. Rev. Lett., 2010, **104**, p. 100601, doi:10.1103/PhysRevLett.104.100601.

Popoff, S. M., Lerosey, G., Fink, M., Boccara, A. C., and Gigan, S., 'Controlling light through optical disordered media: transmission matrix approach,' New Journal of Physics, 2011, **13**(12), p. 123021.

Vellekoop, I. M., 'Feedback-based wavefront shaping,' Opt. Express, 2015, **23**(9), pp. 12189–12206, doi:10.1364/OE.23.012189.

Vellekoop, I. M. and Mosk, A. P., 'Focusing coherent light through opaque strongly scattering media,' Opt. Lett., 2007, **32**(16), pp. 2309–2311, doi:10.1364/OL.32.002309.

Wikipedia, 'S-matrix,' 2018a.

Wikipedia, 'Transfer matrix method - optics,' 2018b.

Yamilov, A., 'Relation between channel and spatial mesoscopic correlations in volume-disordered waveguides,' Phys. Rev. B, 2008, **78**, p. 045104, doi: 10.1103/PhysRevB.78.045104.

Yaqoob, Z., Psaltis, D., Feld, M. S., and Yang, C., 'Optical phase conjugation for turbidity suppression in biological samples,' Nature Photonics, 2008, **2**, p. 110.

Yeh, P., *Optical Waves in Layered Media*, Wiley-Interscience, 2005, ISBN 0471731927.

Yuli V. Nazarov, Y. M. B., *Quantum Transport*, Cambridge University Pr., 2009, ISBN 978-0-521-83246-5.

VITA

Jayson Robert Summers received his B.S. in Physics from Missouri University of Science and Technology in May 2017. In December 2018, he also received his M.S. in Physics from Missouri University of Science and Technology. During his graduate career, Jayson served as a teaching assistant for two courses. In Intermediate Physics Lab, Jayson acted as a laboratory instructor, giving students hands on experimental instruction in power supplies, function generators, oscilloscopes, filters, pulse counters, and other scientific equipment. In Physical Mechanics Lab, he directed students in experiments regarding precision measurement, mechanical energy, conservation of momentum, torque, pressure, and other physics concepts.